

Review

# Recent Progress in Daytime Radiative Cooling: Is It the Air Conditioner of the Future?

Mattheos Santamouris \* and Jie Feng

Faculty of Built Environment, University of New South Wales, Sydney, NSW 2052, Australia;  
jie.feng@unsw.edu.au

\* Correspondence: m.santamouris@unsw.edu.au; Tel.: +61-2-93850729

Received: 4 November 2018; Accepted: 28 November 2018; Published: 30 November 2018



**Abstract:** Radiative cooling is a well-researched area. For many years, surfaces relying on radiative cooling failed to exhibit a sub-ambient surface temperature under the sun because of the limited reflectance in the solar spectrum and the reduced absorptivity in the atmospheric window. The recent impressive developments in photonic nanoscience permitted to produce photonic structures exhibiting surface temperatures much below the ambient temperature. This paper aims to present and analyze the main recent achievements concerning daytime radiative cooling technologies. While the conventional radiative systems are briefly presented, the emphasis is given on the various photonic radiative structures and mainly the planar thin film radiators, metamaterials, 2 and 3D photonic structures, polymeric photonic technologies, and passive radiators under the form of a paint. The composition of each structure, as well as its experimental or simulated thermal performance, is reported in detail. The main limitations and constraints of the photonic radiative systems, the proposed technological solutions, and the prospects are presented and discussed.

**Keywords:** daytime radiative cooling; photonic coolers; plasmonic coolers

## 1. Introduction

Global and local climate change increase the ambient temperature and the frequency, duration, and magnitude of extreme heat events [1]. During the summer period, high ambient temperatures combined with the poor design of buildings and the potentially high internal gains, increase significantly indoor air temperatures. Overheating of the indoor and outdoor built environment has a severe impact on thermal comfort, human health, energy consumption for cooling, peak electricity demand, and the local and global economy [2]. Air conditioning of indoor spaces and mitigation of the outdoor ambient heat are among the most common and acceptable ways to counteract overheating in the built environment.

In some countries, building consumes more than one-third of the total energy [3], among which 1.24 PWh per year was consumed for cooling purposes [4]. This corresponds to about 3.9% of the total energy consumption of the sector [4]. Residential buildings consume around 0.68 PWh/year or 2.9% of the total residential energy consumption, while the consumption of the commercial sector is slightly lower, corresponding to 0.57 PWh/year or 6.7% of the energy spent by the commercial buildings. Air conditioning industry is rapidly expanding reaching a total turnover exceeding 100 billion USD per year [5]. Forecasts of the future energy consumption of the building sector predict that beyond 2050 cooling will be the dominant energy use and will exceed highly the heating demand and consumption [6].

Several technological, social and economic drivers influence and finally define the present and future cooling energy consumption of buildings. Among others, climate change, the increase of the global population, the rise of the expected household income and the housing size, the specific

efficiency of the cooling equipment and the energy performance of buildings are the main parameters to be considered [7]. There is a considerable number of studies forecasting the future cooling energy consumption of the building sector [4,6,8–18]. Although the assumptions and the boundary conditions considered by the various studies differ considerably, there is a common conclusion: the future residential and commercial cooling demand will increase tremendously. Predictions of the residential and commercial cooling demand for 2050 [4], reveal that in the commercial sector the annual cooling energy needs may vary between 0.9 PWh and 2.61 PWh with the most probable value close to 1.5 PWh. This corresponds to an average increase close to 260% compared to the current consumption. The most probable cooling consumption of the residential sector in 2050 is predicted close to 5.3 PWh, corresponding to an increase close to 780% compared to the current residential cooling consumption [4]. The global increase in the use of air conditioning will be driven in particular by some regions. For instance, although the actual share of cooling in electricity peak demand of India is close to 10.5%, it may increase up to 44.1% in 2050 [19].

Conventional air conditioning technologies are associated with important energy, environmental, economic and social problems. Air conditioning causes a serious increase of the peak electricity demand that obliges utilities to build additional power plants and increase the average cost of electricity [20]. It is the source of important indoor air quality and global environmental problems like the ozone depletion and the release of additional heat in the ambient environment [21], intensifying urban overheating. Moreover, the additional cost of electricity consumed for cooling purposes can be a serious burden for low and average income population [22]. Low-income households live in less thermally protected houses requiring a much higher energy demand for heating and cooling [23]. As mentioned in [24], while the average annual cost of air conditioning in Greece is close to 100 Euros per household, low-income families must spend almost the double, 195 Euros, to satisfy their cooling demands. As a result, households are exposed to extreme indoor temperatures exceeding the comfort and health thresholds and putting their lives under immediate threat [25].

Several alternative cooling technologies for buildings and outdoor spaces have been developed and some of them have gained a high technological maturity [26]. Technologies can be classified as passive and active, and many of them are based on the development of advanced materials presenting superior thermal and optical properties. Among other, passive cooling technologies for buildings and outdoor spaces including infrared reflecting materials [27], fluorescent surfaces [28], thermochromic materials [29], and photonic and plasmonic radiative coolers [30], seem to be the most advanced ones presenting a very high cooling potential (Figure 1). Caloric materials including elastocaloric, magnetocaloric, and electrocaloric devices have attracted a very high interest while prototype heat pumps of reasonably high efficiency are already designed and developed [31].

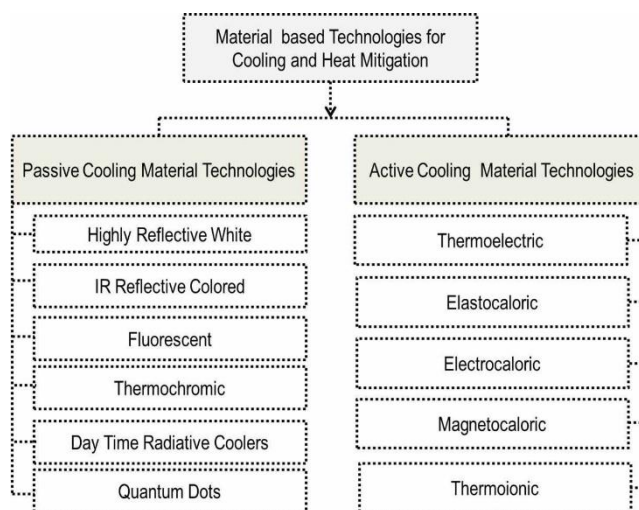


**Figure 1.** Classification of Materials for passive and active cooling.

Radiative cooling is a very well-known cooling technique as it was used during the ancient time to produce ice and cool spaces. It is based on the potential of the terrestrial structures to dissipate heat to the low temperature of 3 °C on their outer surface. Terrestrial structures emit radiative heat at wavelengths where the atmosphere is quite transparent (8–13 μm), while they absorb shortwave and longwave radiation out of the atmospheric window. Once the radiative balance of an emitting surface is negative, its surface temperature may be substantially lower than the ambient one provided that the convective gains are limited. Cool radiators can be used as low-temperature heat exchangers to provide cooling into the buildings [32,33]. Some are also integrated with solar heating to provide both solar heating and radiative cooling [34,35].

Past research on radiative cooling has resulted in the development of several technologies including among others selective surfaces, thin films, reflective covers, presenting a substantial high reflectivity in solar radiation and a high emissivity in the atmospheric window [36]. Although during the night period almost all the above technologies succeed to exhibit a very significant cooling potential, during the daytime their cooling capacity is almost negligible as their surface temperature fails to be lower than the ambient one. Given that buildings require cooling during the peak day period, the development of daytime sub-ambient radiative technologies was the ultimate objective of the related research.

Recent Intensive research mainly carried out on advanced photonic and plasmonic surface technologies has resulted in the development of sub-ambient daytime radiative coolers [37–42]. The developed technologies seem to provide a very high daytime cooling capacity that may contribute highly to decrease the current and future cooling demand of buildings. This article aims to present the recent developments in the field of daytime radiative cooling, the various developed surface technologies, their main advantages and drawbacks, and finally their potential to provide cooling in the built environment.

## 2. Fundamentals of Radiative Cooling

The cooling potential of a radiative cooler is a direct function of its surface temperature,  $T_c$  (K). The higher the depression of the surface below the ambient air temperature,  $T_a$  (K), the higher the cooling potential of the cooler. The cooling flux of a radiative cooler,  $Q_{rc}$  ( $W/m^2$ ), is a function of the absorbed shortwave radiation,  $E_{sw}$  ( $W/m^2$ ), the emitted longwave radiation by the cooler,  $E_{rlw}$  ( $W/m^2$ ), the absorbed longwave radiation,  $E_{alw}$  ( $W/m^2$ ), and of the convective heat gains/losses,  $Q_{cl}$  ( $W/m^2$ ):

$$Q_{rc}(T_c, T_a) = E_{sw} + E_{alw}(T_a) - E_{rlw}(T_c) + Q_{cl} \quad (1)$$

The absorbed short wave radiation,  $E_{sw}$  is a function of the incident total solar radiation on the radiator surface, the broadband absorptivity,  $\alpha_{sr}$ , of the surface in the solar wavelength range and the broadband transmissivity of a potential cover at the same wavelengths,  $\tau_{sc}$ . Calculations can be performed using the spectral irradiance distribution,  $I(\lambda)$  ( $W/m^2/nm$ ), and the corresponding spectral absorptivity  $\alpha_{sr}(\lambda)$ ,  $\tau_{sc}(\lambda)$ .

$$E_{sw} = \int_0^{\infty} I(\lambda) \alpha_{sr}(\lambda) \tau_{sc}(\lambda) d\lambda \quad (2)$$

The atmospheric radiation is the result of the specific emission of each atmospheric constituent and in particular of water vapor, carbon dioxide, ozone, hydrocarbons and nitrogen oxides. The atmospheric radiation absorbed by the radiator,  $E_{alw}(T_a)$ , depends on the intensity of the infrared radiation emitted by the atmosphere, the transmissivity of the cover in the specific infrared wavelengths,  $\tau_{rc}(\lambda, \theta)$ , and also the absorptivity/emissivity  $\alpha_{ir}(\lambda, \theta)$  of the radiator in the same waveband. Where  $\theta$  is the zenith angle.

$$E_{alw}(T_a) = \int_0^{\pi/2} \int_0^{\infty} I_{bb}(\lambda, T_a) \alpha_{sr}(\lambda, \theta) \tau_{rc}(\lambda, \theta) \varepsilon_a(\lambda, \theta) 2\pi \sin \theta \cos \theta d\theta d\lambda \quad (3)$$

where  $I_{bb}(\lambda, T_a)$  is the blackbody spectral intensity, and  $\epsilon \alpha$  is the spectral emittance of the atmosphere. A review of the proposed expressions to calculate the emittance of the atmosphere is given in [30,36].

The radiative flux emitted by the surface,  $E_{rlw}(T_s)$ , is a function of the surface temperature and of the spectral emissivity of the radiator,  $\epsilon_{sr}(\lambda, \theta)$ .

$$E_{rlw}(T_s) = A \int d\Phi \cos \theta \int d\lambda I_{bb}(T, \lambda) \epsilon_{sr}(\lambda, \theta) \quad (4)$$

where  $\int d\Phi$  is the angular integral over the hemisphere.

Finally, the convective heat losses,  $Q_{cl}$  are:

$$Q_{cl} = Ah(T_c - T_a) \quad (5)$$

### 3. Conventional Radiative Cooling Technologies

Ideal materials for radiative cooling should present: (a) The maximum possible reflectivity in the short-wave range (0.25–2.8  $\mu\text{m}$ , with the majority of the solar power available between 0.3 and 2.2  $\mu\text{m}$ ); and (b) emissivity in the atmospheric window band close to unity (8–13  $\mu\text{m}$ ) and zero in the rest of the thermal wavelength range (4–80  $\mu\text{m}$ ). Past research on radiative cooling was aiming at identifying natural or creating composite materials of such properties, at least as close as possible. Research was oriented towards the use of commercially available polymers, metals, gases, or simply synthesized composite materials to form a radiative cooler. The dependency on inherent properties of natural or composite materials or, in other words, the incapability to precisely control their optical spectrum significantly limits the cooling performance. In fact, very few structures achieved sub-ambient results in daytime conditions. Most of the proposed structures can only demonstrate a sub-ambient surface temperature only during the night period. In the following, the main proposed conventional radiative cooling structures are briefly presented and reviewed. The review covers both the radiative cooler itself and the commonly used shields on top of the cooler to reduce convective losses and increase reflectivity to solar radiation.

#### 3.1. Selective Coolers

TiO<sub>2</sub> white paints have usually both high emittance ( $\geq 0.92$ ) in the 8–13  $\mu\text{m}$  spectral region and high solar reflectivity (Peak solar reflectance  $\geq 0.95$ ) [43]. By painting a commercially available high content TiO<sub>2</sub> to an aluminum substrate, Harrison and Walton [44] achieved a 2 °C sub-ambient surface temperature at noon under direct sunlight. Orel et al. [45] found that when in the mixture of TiO<sub>2</sub> and BaSO<sub>4</sub>, barium sulphate is added, the performance of TiO<sub>2</sub> white pigment as infrared selective radiator can be slightly improved due to SO<sub>4</sub> stretching vibrations of the BaSO<sub>4</sub> extender. However, the difference of the temperature drop between paints containing BaSO<sub>4</sub> and those without it did not exceed 3.2 °C.

Catalanotti et al. [46] coated a sheet of aluminum with a polyvinyl-fluoride thin film (thickness: 12  $\mu\text{m}$ ) from TEDLAR, DuPont. According to Tsilingiris [47] and Gutpa and Tandon [48], this film has particularly high absorptance in the atmospheric window band but also an absorption peak around 3  $\mu\text{m}$ . When incorporated with aluminum as a solar reflector, this selective radiator can have a desired selective spectrum except the huge dip of solar reflectivity exactly around 3  $\mu\text{m}$ . During the daytime, it can reach up to 15 °C below the ambient temperature when shielded from direct solar radiation. Other similar attempts included the use of polyvinylchloride (PVC) [49] and poly(4-methylpentene)(TPX) [50], but due to their high absorption outside the atmospheric window they are less suitable for radiative cooling purposes [36,51].

Hjortsberg and Granqvist [52] investigated the radiative properties of ethylene (C<sub>2</sub>H<sub>4</sub>). Due to out-of-plane bending vibrations of the molecules, it has two strong absorption bands matching the atmospheric window range. When the gas slabs are backed with opaque aluminum layers, they can reach under clear sky up to 10 °C sub-ambient temperature with direct sunlight blocked. Lushiku [53],

and Lushiku and Granqvist [54] tested ammonia ( $\text{NH}_3$ ), ethylene ( $\text{C}_2\text{H}_4$ ) and ethylene oxide ( $\text{C}_2\text{H}_4\text{O}$ ). These gases all have a boiling point lying below the normal ambient temperature (i.e.,  $20^\circ\text{C}$ ) and absorb significantly in the  $8\text{--}13\ \mu\text{m}$  range. They concluded that  $\text{NH}_3$  performs the best among the pure gases while the mixture of  $\text{C}_2\text{H}_4$  and  $\text{C}_2\text{H}_4\text{O}$  allows the biggest temperature drop. Being readily available substances, gases do not need expensive coating technology and can serve as heat-transfer fluid in a practical device. Neither the purity nor the thickness of the gas slab impact its performance significantly, but it always need to be sealed by an infrared-transparent material which might limit the application.

Granqvist and Hjortsberg [55,56] investigated  $\text{SiO}$  films on Al as selective surfaces for radiative cooling and tested the spectral radiative properties of such surface in different thickness. They found that when the film thickness of  $\text{SiO}$  is close to  $1\ \mu\text{m}$ , the combination of its lattice absorption band and destructive interference will lead to high emittance in the atmospheric window band. A surface temperature of at least  $40\ \text{K}$  below the ambient was computed. Granqvist et al. [57] studied  $\text{SiO}$  and  $\text{Si}_3\text{N}_4$  films in small scale experiments. At clear nights,  $\text{SiO}$  coated aluminum surface reached minimum  $14^\circ\text{C}$  below the ambient temperature. Since the absorption band of  $\text{Si}_3\text{N}_4$  covers the atmospheric window range wider than  $\text{SiO}$ , it was supposed to present a better performance; however this has not been proved experimentally. The optical properties of silicon nitride thin films for radiative cooling are also investigated by Eriksson et al. [54,58,59] and Zongcun et al. [60]. They found that the cooling performance of oxynitride is superior to that offered by nitride/dioxide bilayers. Using nano-particles, Miyazaki [61] even synthesized  $\text{Si}_2\text{N}_2\text{O}$  and coated it to Al substrates. The temperature of the  $6.5\text{-}\mu\text{m}$ -thick film and  $13.5\text{-}\mu\text{m}$ -thick film achieved an average  $0.82^\circ\text{C}$  and  $0.44^\circ\text{C}$  temperature drop below the ambient air temperature. A similar study using silicon oxynitride was conducted by Diatezua et al. [62] and a sub-ambient temperature was predicted.  $\text{SiO}_2$  and  $\text{SiC}$  are also candidates for radiative cooling as their phonon resonances lead to high IR emission. Gentle and Smith [63] reported a temperature of maximum  $17^\circ\text{C}$  below the ambient air at night generated by doping crystalline  $\text{SiC}$  and  $\text{SiO}_2$  nanoparticles on aluminum.

Tazawa et al. [64,65] added a transition metal oxide thermochromic film to their design as it shows significant change of its reflectivity when the phase changes at a certain temperature [66]. They produced a radiative material which used a  $\text{SiO}$  film at the top layer and  $\text{V}_{1-x}\text{W}_x\text{O}_2$  thermochromic film beneath it. It can reach a stable temperature lower than the ambient one and this temperature can be controlled by the value  $x$  in  $\text{V}_{1-x}\text{W}_x\text{O}_2$ .

For a given medium, if there is change in refractive index together with the specific absorption band, electromagnetic radiation within this band cannot propagate within it which is called the reststrahlen effect. Being unable to propagate, strong-reflection or total-reflection in a reststrahlen band can be observed [67].  $\text{MgO}$  is exactly such a medium. Due to the strong reststrahlen reflectivity of its ceramic form at wavelengths  $> 13\ \mu\text{m}$ , if it is backed by a high-solar-reflectivity material, such as a metal film, it can be good a selective radiator with the only low-reflectivity (high emittance) band in  $8\text{--}13\ \mu\text{m}$ . Berdahl [68] has shown experimentally that such a structure, can be  $22^\circ\text{C}$  below the ambient temperature during the night.

### 3.2. Shield for Radiative Cooler

Due to the high transmittance almost all over the spectrum, polyethylene (PE) is the most fundamental material as a shield or the substrate of shield [69]. PE itself can suppress convective heat gain and transmit infrared (IR) emission [70]. But the study of Ali et al. [71] demonstrated that polyethylene foils are heavily impacted by aging. They also concluded that thinner films have better optical radiative but poorer mechanical performance than thinner films. That is why in [72] a polymeric mesh was proposed.

Numerous kinds of shields are proposed for radiative cooling using PE as a substrate. Since  $\text{ZnS}$  and  $\text{ZnSe}$  possess high reflectivity in the solar wavelengths and transmit strongly in the atmospheric window band, they are used by Nilsson et al. [43,73] as pigments for PE convection shields. When using

BaSO<sub>4</sub> as the emitter in 8–13 μm band and with incident solar radiation of approximately 1000 W/m<sup>2</sup>, the radiator was 1.5 K above the air temperature.

Nilsson et al. [43,73] also tested the performance of TiO<sub>2</sub>, ZrO<sub>2</sub> and ZnO. Niklasson and Eriksson [74] analyzed the reflectivity and transmittance of TiO<sub>2</sub> pigmented polyethylene foils with different volume fractions of TiO<sub>2</sub>. Since TiO<sub>2</sub> possess high absorption in part of the atmospheric window band, they are not as superior as ZnS and ZnSe. But if TiO<sub>2</sub> pigment is in nanoscale, its optical characteristics can be influenced significantly by the size effect. Choosing the proper size of nano-particles can lead to desired performance [75].

According to K.D. Dobson et al. [76], deposition of PbS and PbSe films onto polyethylene foils can also act as convective shield for radiative cooling. Although PbS and PbSe have high transmittance (0.508–0.741) in the atmospheric window, they absorb highly in the solar spectrum (solar absorptance is between 0.49–0.636). When incorporated with ZnS and ZnO whose solar reflectivity (peak reflectivity are 0.7–0.85), are relatively high, the final film cannot achieve a satisfactory reflectivity values (peak reflectivity is 0.4) in solar wavelengths [77]. Similar with PbS and PbSe, CdTe [78], CdS [79], and Te [80] thin films have high transmittance (0.62–0.8) across the 8–13 μm band but low solar reflectivity (0.01–0.047). They are supposed to act as good “atmospheric-window material” but considering their high solar absorptance, they are not suited for convection cover in radiative cooling.

Mouhib et al. [81] tested the properties of a stainless steel-tin double layer deposited on glass as a shield for a blackbody radiator. Using glass facing the sky, it can prevent the transmittance of most of the radiation while having a relatively high solar reflectivity (0.517). However, its absorption in 8–13 μm band is too high (over 0.8) for a cover as it may block the emission from the radiator beneath it. Figure 2 shows the transmissivity as well as the absorptivity in the solar spectrum as well as the transmissivity in the atmospheric window of most of the proposed covers for radiative cooling purposes [77].

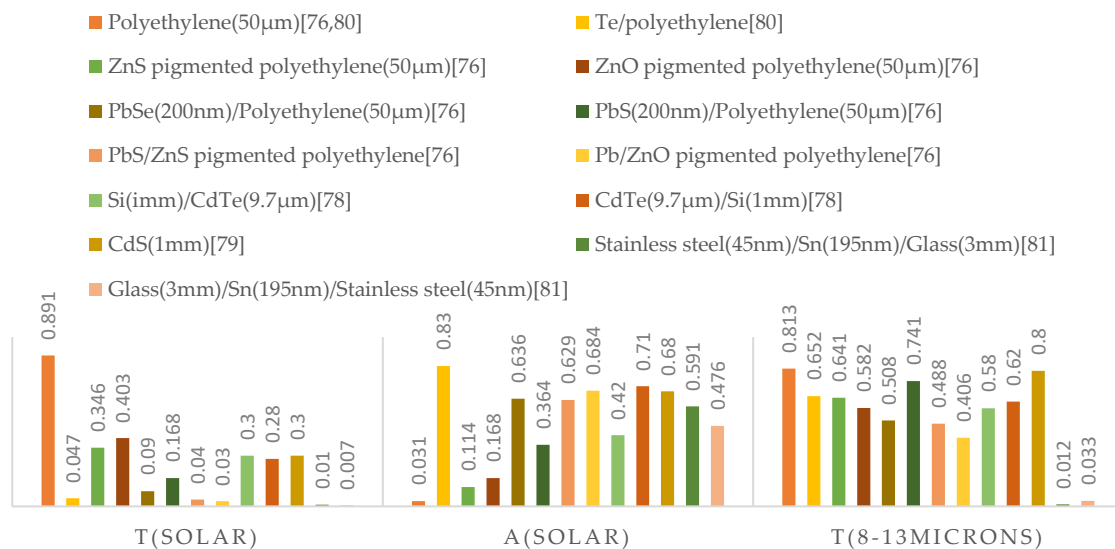


Figure 2. Radiative properties of different shields (T is transmittance and A is absorptance) (Origin: [77]).

The use of natural or composite selective materials succeeds to decrease the surface temperature of the radiator much below the ambient temperature during the nighttime. However, under strong solar radiation, the optical properties of the proposed structures cannot support an operation below the ambient temperature. Given that the cooling demand of commercial and office buildings is mainly during the daytime, the need to develop radiative cooling technologies operating under sub-ambient temperature conditions during the daytime is obvious.

#### 4. Technology Progress on Day Time Radiative Cooling Technologies

Selective natural materials discussed in the previous chapter fail to present a very high reflectivity in the solar spectrum together with a substantially high emissivity in the atmospheric window. As a result, these materials cannot operate below the ambient temperature when sunlit. A successful daytime radiative cooling structure should present a solar reflectivity much higher than 0.9 together with a high emissivity value (i.e.,  $>0.9$ ), in the atmospheric window [38]. Recent advances in the design of optical nanostructures, combined with the significant progress of nanofabrication technologies, offer significant new opportunities to modify the structure of materials at the nanoscale and increase their spectral absorptivity and emissivity to electromagnetic radiation. Several photonic structures like multilayer planar photonic thin films, 2D and 3D photonic devices, metamaterials and plasmonic structures have been proposed and tested to increase as much as possible the emissivity in the atmospheric window in parallel with high reflectivity in the solar range [37–42]. Most of the proposed photonic structures have successfully demonstrated to operate below the ambient temperature during daytime and under high solar radiation intensity.

New designs of lower cost and complexity have been recently proposed based on polymeric photonics [82], as is shown in Figure 3j. The proposed radiators are based on the use of electromagnetic resonators that are collectively excited inside a polymer surface resulting in a very high emissivity in the atmospheric window. Other newly proposed passive systems of radiative cooling like advanced paints, offer a high potential for radiative cooling at considerably low prices [83]. However, optical ageing problems because of the deposition of dust and other atmospheric constituents on the paints as well as unnecessary cooling during the heating period seem to be problems that need to be addressed.

In the following, the recent developments on daytime radiative cooling are presented. Twenty-two proposed daytime radiative structures are analyzed regarding their optical characteristics and thermal performance. Structures are classified in four major technological clusters: (a) Multilayer Planar Photonic Structures; (b) Metamaterials and 2D-3D photonic structures; (c) Polymers for Radiative Cooling and (d) Paints for Radiative Cooling. The main optical characteristics of all the structures as well as their thermal performance are reported in Table 1.

**Table 1.** The main daytime radiative cooling technologies and structures, their composition, optical characteristics and performance.

No	Solar Short Wave Reflective Structure	Reflectivity in Short Wave Solar Radiation (0.3–2 $\mu\text{m}$ )	Emissive Structure	Emissivity in the Atmospheric Window	Day Time Net Cooling Potential ( $\text{W}/\text{m}^2$ )	Day Time Surface Temperature Depression below ambient Temperature ( $^{\circ}\text{C}$ )	Reference
Multilayered Planar Photonic Radiative Structures							
1	Four bottom layers of $\text{HfO}_2$ , $\text{SiO}_2$ , $\text{HfO}_2$ , $\text{SiO}_2$ , on top a silver mirror	0.97	Three upper layers of $\text{SiO}_2$ , $\text{HfO}_2$ , $\text{SiO}_2$ on top of the structure.	Varies between 0.5–0.8	40.1 (experimental)	5 $^{\circ}\text{C}$ (experimental)	[70]
2	Metal film and reflective substrate	Not Reported	Layers of polar materials like SiC and BN	0.9–1	Not Calculated or measured	Not Calculated or measured	[84]
3	Al Mirror/Radiator under vacuum	Not Reported	Two layers of Si and $\text{Si}_3\text{N}_4$	Varies between 0.2–0.9	Not reported	Maximum: 42 $^{\circ}\text{C}$ Not below 33 $^{\circ}\text{C}$ during the day time	[39]
4	A layer of suboptimum $\text{TiO}_2$ particles and an Al mirror	0.907	$\text{SiO}_2$ particles	0.901	Not Reported	Surface Temperature above ambient temperature	[85]
5	Silver film	0.9	Fused silica wafer coated in its top with PDMS	0.9–1.0	127 (Experimental)	8.2 $^{\circ}\text{C}$ (Experimental)	[41]
6	4 bottom alternate layers of $\text{SiO}_2$ and $\text{TiO}_2$ above a silver mirror	0.97	Alternative layers $\text{TiO}_2$ , $\text{SiO}_2$ , and $\text{Al}_2\text{O}_3$	0.7–0.8	85.5 (Simulation)	Not calculated	[86]
7	Silver Film	0.9	Layers of $\text{HfO}_2$ , BN, SiC and $\text{SiO}_2$ and lamellar gratings of SiC, $\text{SiO}_2$ and BN	0.5–1.0	40 (Simulation)	Not calculated	[87]
8	11 layers of Ge/ $\text{MgF}_2$	Transmissivity below 0.1	Three layers of $\text{VO}_2$ , $\text{MgF}_2$ and W	0.8–1.0	Not Reported	9 (Simulation)	[88]
Metamaterials and 2D-3D Photonic Structures							
9	Three sets of 5 bilayers of $\text{MgF}_2$ and $\text{TiO}_2$ over a silver substrate.	0.965	Two 2D layers of SiC and Quartz	0.1–0.95	105 (Simulation)	8 $^{\circ}\text{C}$ or 15 $^{\circ}\text{C}$ for a heat transfer coefficient 12 or 6 $\text{W}/\text{m}^2/^{\circ}\text{C}$ respectively	[89]
10	A conical metamaterial composed by symmetrically shaped conical metamaterial pillars composed by alternating layers of aluminium and germanium	0.97	A conical metamaterial composed by symmetrically shaped conical metamaterial pillars composed by alternating layers of aluminium and germanium	0.99	Not reported	9 $^{\circ}\text{C}$ (simulated)	[90]
11	Not mentioned	Not mentioned	A 2D SiC metasurface	0.25–0.75, average = 0.6	Not tested or simulated	Not tested or simulated	[91]
12	An array of dielectric resonators coated with a silver layer	0.97	The typical cell of the metasurface consists of a doped silicon substrate and to rectangular dielectric resonators placed orthogonally to each other and coated in their top with silver	0.8–0.95	96 (Simulated)	8.2 $^{\circ}\text{C}$ (Simulated)	[42]
13	Micropyramids composed by 19 alternate $\text{Al}_2\text{O}_3/\text{SiO}_2$ pairs of variable length thin film with a silver layer at the bottom.	0.95	Micropyramids composed by 19 alternate $\text{Al}_2\text{O}_3/\text{SiO}_2$ pairs of variable length thin film	0.65–1	122 (Simulated)	Not Reported	[92]
Polymers for Radiative Cooling							
15	Al film	0.9	Crystalline SiC and $\text{SiO}_2$ nanoparticles are used to dope a 25- $\mu\text{m}$ thick PE, transparent to IR radiation	0.35–0.95	Not Reported	12–25 $^{\circ}\text{C}$ (Simulation)	[63]
16	Two polymers on top and a silver film on the bottom	0.97	Two polymers	0.96	Not reported	2 $^{\circ}\text{C}$ without convective protection (Experimental)	[38]

Table 1. Cont.

No	Solar Short Wave Reflective Structure	Reflectivity in Short Wave Solar Radiation (0.3–2 $\mu\text{m}$ )	Emissive Structure	Emissivity in the Atmospheric Window	Day Time Net Cooling Potential ( $\text{W}/\text{m}^2$ )	Day Time Surface Temperature Depression below ambient Temperature ( $^{\circ}\text{C}$ )	Reference
17	Acrylic resin is embedded with $\text{TiO}_2$ nanoparticles	0.90	Acrylic resin embedded with carbon black particles	0.9	100 (simulated)	6 $^{\circ}\text{C}$ (Simulated)	[40]
18	Silver Coating	0.96	A transparent polymer where randomly distributed silicon dioxide microspheres. The polymer is 50- $\mu\text{m}$ thick and includes 6% of microspheres.	0.93	93 (Experimental)	Not Reported	[82]
19	A highly reflective polymer on top of a silver film	0.97	A polymer	0.96	Not Reported	Decrease of the water temperature in contact with the radiator up to 5 $^{\circ}\text{C}$ below the ambient temperature (experimental)	[33]
20	Silver Coating	0.95	A transparent polymer where randomly distributed silicon dioxide microspheres. The polymer is 50- $\mu\text{m}$ thick and includes 6% of microspheres	0.86		Decrease of the water temperature in contact with the radiator up to 10.6 $^{\circ}\text{C}$ below the ambient temperature (experimental)	[93]
Paints for Radiative Cooling							
21	Low refractive index microspheres of $\text{SiO}_2$	0.97	Microspheres of $\text{SiO}_2$	0.95	Not reported	12 $^{\circ}\text{C}$ (experimental)	[83]
22	An hierarchically porous poly(vinylidene fluoride-cohexafluoropropene) (P(VdF-HFP)HP) coating	0.96	An hierarchically porous poly(vinylidene fluoride-cohexafluoropropene) (P(VdF-HFP)HP) coating	0.97	96 (Experimental)	6 $^{\circ}\text{C}$ (Experimental)	[94]

#### 4.1. Multilayer Planar Photonic Radiative Structures

Multilayer planar photonic radiative structures are composed by two main parts aiming to increase the reflectivity of the structure in the short wavelength range (0.3–2.5  $\mu\text{m}$ ), and to enhance the absorptivity of the structure in the atmospheric window (8–13  $\mu\text{m}$ ).

To achieve a high reflectivity in the shortwave, either a single Ag or Al mirror is used [39,41,84,87,95], or a structure of alternate layers of high and low refraction index materials [87], or a combination of a Ag or Al mirror on the bottom of alternate high–low refractive index materials [70,85,86]. The specific composition of the reflective component of each structure is described in Table 1. When a single Ag or Al reflector is used, the achieved reflectivity in wavelengths between 0.3 to 2.5  $\mu\text{m}$  is close to 0.9 for the structures reported in [87,95]. The structure proposed in [88] presents a very low transmissivity in the shortwave wavelength, below 0.05, mainly because of the high absorptivity of Ge. Much higher reflectivity values, between 0.97 and 0.98, are measured when a metal reflector is combined with a thin film of alternating materials of high and low refractive index [70,86]. In [70], layers of  $\text{SiO}_2$  and  $\text{HfO}_2$  are used, while in [86],  $\text{HfO}_2$  is replaced by  $\text{TiO}_2$ , as is shown in Figure 3a.

To enhance the absorptivity of the structure in the atmospheric window films composed by one up to 4 different materials are used (Table 1). Most structures are designed to exhibit phonon–polariton excitation in the atmospheric window. The resulting spectral emissivity depends mainly on the specific wavelengths that the material resonates and the number of the layers used. In [85], a single layer of  $\text{SiO}_2$  is used, as is shown in Figure 3h and the calculated emissivity in the atmospheric window was close to 0.9. In [13,39,41,70,81,84], a combination of two materials is projected. In [41], a fused silica wafer of 500- $\mu\text{m}$  thickness, coated in its top with 100- $\mu\text{m}$  thick PDMS is proposed, as is shown in Figure 3e. The structure presents a high emissivity in the atmospheric window (AW) (0.9–1), but also a high emissivity in the infrared spectrum out of the atmospheric window. In [70], alternating layers of  $\text{SiO}_2$  and  $\text{HfO}_2$  are used and the emissivity in the atmospheric window varied between 0.5 and 0.8, as is shown in Figure 3c. In [84], layers of  $\text{SiO}_2$  and BN are proposed and the average emissivity in the AW found to vary between 0.9–1. In [95],  $\text{SiO}_2$  is combined with PPMA giving an average emissivity in the AW close to 0.72, while in [39], layers of Si and  $\text{Si}_3\text{N}_4$  are used and the spectral emissivity in the AW varied between 0.2 to 0.9. In [86,88], the emitting structures were composed by three different materials. In [86], alternating layers of  $\text{TiO}_2$ ,  $\text{SiO}_2$  and  $\text{Al}_2\text{O}_3$  were proposed and the emissivity in the AW was between 0.7 and 0.8. In [88], layers of  $\text{VO}_2$ ,  $\text{MgF}_2$  and W were proposed resulting in an emissivity in the AW between 0.8 to 1.0. Finally, in [87], the emitting structure was composed by layers of four different materials,  $\text{HfO}_2$ , BN, SiC and  $\text{SiO}_2$ , in combination with Lamellar grating of SiC,  $\text{SiO}_2$  and BN. The resulting spectral emissivity in the AW varied between 0.5 and 1. In all proposed structures, except in [85,88], the emitting layers were placed above the reflecting ones. In this case, the layers on top should present a very high transmissivity in the short wavelength solar radiation to allow effecting reflection of the solar radiation. In [85,88], the emitting layers were placed on the bottom of the thin film. In this case, the upper layers of the film should present a very high transmissivity in the radiation emitted by the lower structure in the atmospheric window wavelengths.

The thermal performance of the radiative structures during the daytime has been assessed either experimentally [39,41,70,85,95] or through simulation [86–88] (Table 1). The net cooling power as well as the surface temperature of the radiators, depends on the optical characteristics reported above, the atmospheric content and the associated atmospheric radiation in the specific place and the convective–conductive gains/losses of the radiator. In areas presenting high humidity content, the atmospheric window between 16 and 25  $\mu\text{m}$  is quite closed, resulting in a higher absorption of atmospheric radiation by the radiator. Measurements of the thermal performance of multilayered planar photonic radiative coolers performed in areas of high humidity [85,95], shown that the radiator surface temperature fails to be below the ambient one during the daytime. As discussed in the previous sections, conductive and convective losses highly influence the thermal performance of the radiative coolers. In [39], the convective/conductive losses/gains were minimized by positioning the radiative

cooler under vacuum conditions. Measurements show that the daytime surface temperature of the cooler was reduced up to 42 °C below the ambient temperature, while during the whole daytime it was kept up to 33 °C lower than the ambient temperature. Testing of a multilayered photonic radiative cooler under ambient conditions in a relatively dry area and using a structure to reduce the convective losses is reported in [70]. The surface temperature of the radiator was reduced during the daytime up to 5 °C below the ambient temperature, while the cooler presented a net cooling power close to 40 W/m<sup>2</sup>. Experimental testing of the radiator proposed in [41], shown that its daytime surface temperature was 8.2 °C below the ambient temperature. Its net cooling power was estimated close to 127 W/m<sup>2</sup>. The simulated net cooling power of the radiators proposed in [86] and [87], were close to 85 W/m<sup>2</sup> and 40 W/m<sup>2</sup> respectively, while the potential daytime temperature drop of the radiator proposed in [88], was close to 9 °C. Given the high diversity between the testing conditions and the simulation assumptions, it is impossible to compare the performance reported for the different radiative coolers.

#### 4.2. Metamaterials and 2D-3D Photonic Structures

Boosting the emission of light in the infrared wavelength area using photonic structures has been experimentally and theoretically proved using two- and three-dimensions photonic crystals and metamaterials. Although planar photonic devices may present a very high reflectivity in the shortwave range, they do not present a very high emissivity in the whole spectrum of the atmospheric window. Two- and three-dimension structures can provide a very high reflectivity in combination with a high emissivity in the atmospheric window. Metamaterials can support in parallel lattice and local resonance modes that permit to optimize the emissivity in the desired spectrum and increase the cooling capacity. However, they require complicated and relatively expensive microfabrication that decreases the scalability of the structures. Several configurations of 2D and 3D photonic structures and metamaterials have been proposed and tested. Some of the most important proposed structures are analyzed below (Table 1).

In [92], a metamaterial structure based on multilayer all dielectric micro-pyramid structure is proposed, as is shown in Figure 3b. The structure was designed to enhance its absorption performance in the atmospheric window compared to single plane photonic devices. The micro-pyramids are composed by 19 alternate Al<sub>2</sub>O<sub>3</sub>/SiO<sub>2</sub> pairs of variable length thin film with a silver layer at the bottom. All thin films were below 7.5 μm length to ensure that operate like a sub-wavelength structure. The thickness of the Al<sub>2</sub>O<sub>3</sub> and SiO<sub>2</sub> layers were 2 μm and 1 μm respectively. Calculations of the optical properties of the structure shown that its emissivity in the atmospheric window is approaching one, mainly because of the gradual change of the refractive index and not because of the light trapping effect like in the multilayered metal -dielectric structures. The calculated optical properties in the atmospheric window are considerably higher than the reported for other metamaterial structures and vary as a function of the SiO<sub>2</sub> layer. The emissivity in the atmospheric window is calculated to vary between 0.65 and 1. The absorptivity of the structure in the solar spectrum was also very close to zero. Numerical simulations shown that the proposed radiative cooler can achieve a cooling power up to 122 W/m<sup>2</sup>. Although the proposed structure presents superior optical properties, it requires a quite complicated manufacturing process involving either a nano imprint physical vapor deposition, or a layer by layer fabrication.

In [42], dielectric resonator metasurfaces are used for daytime radiative cooling. The metasurface consists of an array of dielectric resonators coated with a silver layer. The radiator is based on the use of the magnetic dipole resonance of the dielectric resonators to increase the absorptivity and emissivity at wavelengths that match the atmospheric window. The radiator is composed of two materials: silver and phosphorous-doped n-type silicon. The typical cell of the metasurface consists of a doped silicon substrate and the rectangular dielectric resonators placed orthogonally to each other and coated in their top with silver. The emissivity of the metasurface in the atmospheric window was measured between 0.80 and 0.95. Based on calculations, it is reported that the maximum nighttime cooling power was 96 W/m<sup>2</sup>, and the maximum night time depression close to 11.4 °C below the ambient

temperature. The calculated daytime temperature depression was 8.25 °C. The proposed radiator presents a structural simplicity, low material cost and a scalable fabrication. However, the fabrication of the radiator requires use of nanofabrication processes like electron bin lithography and plasma enhanced deep reactive ion etching, as well as electron bin deposition of the metal.

In [89], a 2D metal dielectric photonic structure for daytime radiative cooling is presented, as is shown in Figure 3f. The system consists of a thermally selective emitter on top of a broadband mirror. The reflector is composed of three sets of 5 bilayers of MgF<sub>2</sub> and TiO<sub>2</sub> over a silver substrate. The emitter is composed of two 2D layers of SiC and Quartz. Both materials used in the emitter present a strong resonance in the atmospheric window, Quartz at 9.3 μm and SiC at 12.5 μm. The structure is making use of the phonon-polariton phenomenon to enhance emissivity in the atmospheric window. Simulations have shown that the proposed photonic structure is able to achieve a maximum net cooling power close to 105 W/m<sup>2</sup>, and a daytime temperature suppression close to 8 °C below the ambient temperature for a heat transfer coefficient close to 12 W/m<sup>2</sup>/°C or 15 °C, for an h = 6 W/m<sup>2</sup>/°C. Fabrication of the proposed photonic cooler requires techniques like nanoimprint lithography. The radiator has not been tested experimentally in outdoor conditions.

In [91], the use of silicon carbide metasurfaces presenting a high selective emissivity in the atmospheric window mediated by magnetic polaritons, is presented. Magnetic polaritons state the intensive coupling of external electromagnetic waves with the magnetic resonance in the nanostructures that results in a control of radiative properties. A 2D SiC metasurface has been tested and it is found that the emissivity in the atmospheric window varies between 0.2 and 1 with an average value close to 0.6.

In [90], an anisotropic conical metamaterial composed by symmetrically shaped conical metamaterial pillars is proposed, as is shown in Figure 3d. The pillars are composed of alternating layers of aluminum and germanium. The structure presents an emissivity in the atmospheric window close to 99%, while calculations estimate that the radiator may succeed to achieve 9 °C below the ambient temperature during the daytime.

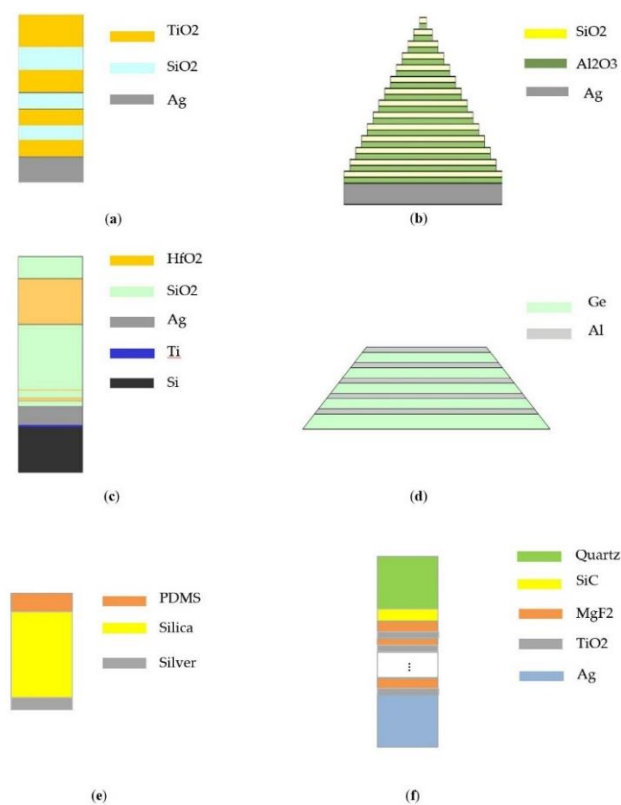
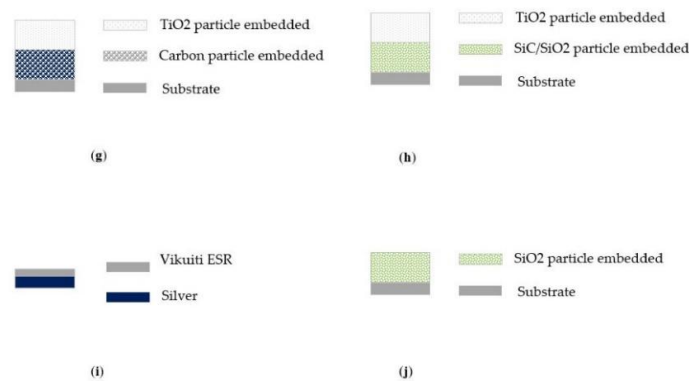


Figure 3. Cont.



**Figure 3.** Schemes of some photonic structures. (a) 50 nm thick Ag is coated on Si substrate. Then, 4 alternative layers of TiO<sub>2</sub> and SiO<sub>2</sub> are added, and the thickness of each layer is 60 nm. Then 3 layers of TiO<sub>2</sub> and SiO<sub>2</sub> are added, each 300 nm thick [86]. (b) Radiative cooler of multilayer pyramidal nanostructure. The thickness of each SiO<sub>2</sub> layer is 1 μm and of each Al<sub>2</sub>O<sub>3</sub> layer is 2 μm [92]. (c) This photonic structure consists of 7 layers of SiO<sub>2</sub> and HfO<sub>2</sub>, on top of 200 nm thick Ag, 20 nm thick Ti and 750-μm thick Si substrate [70]. (d) A thermal emitter with multilayer arrays of symmetrically shaped conical metamaterial pillars. The thickness of aluminum layer is 30 nm and the thickness of germanium layer is 110 nm [90]. (e) A polymer silica mirror is produced by coating a 500 μm thick fused silica wafer with a 100-μm thick PDMS film on top and 120 nm thick silver film to reflect on the back [41]. (f) The radiative cooler consists of 2 photonic crystal emitters comprised of quartz and SiC. The reflector lies below the emitters contains three sets of five bilayers made of MgF<sub>2</sub> and TiO<sub>2</sub>. Silver serves as a substrate [89]. (g) A double layer coating with TiO<sub>2</sub> embedded on top and carbon black on bottom [40]. (h) A double layer coating with TiO<sub>2</sub> embedded on top and SiC or SiO<sub>2</sub> on bottom [85]. (i) Vikuiti Enhanced Specular Reflector (ESR) is all polyester and believed to consist of PET/ECDEL pairs with ECDEL a Kodak copolyester. The back surface is coated with silver [38]. (j) The metamaterial consists of a transparent polymer with randomly distributed SiO<sub>2</sub> microspheres [82]. (Origin of a,c,e,f,g,h,i,j:[30]).

#### 4.3. Polymers for Radiative Cooling

Polymeric photonics is an attractive solution for daytime radiative cooling. Polymers are doped with nanomaterials-resonators, that are collectively excited resulting in a high absorptance emissivity in the atmospheric window wavelengths where nanoparticles resonate [40,63,82,93]. In [63], it was proposed to dope a 25-μm thick PE with crystalline SiC and SiO<sub>2</sub> nanoparticles. The emissivity value in the atmospheric window was varying between 0.35 and 0.95. In [40], carbon black particles were embedded in an acrylic resin to enhance thermal emission in the atmospheric window, as is shown in Figure 3g. The average emissivity in the atmospheric window was close to 0.9. In [82,93], the emissive structure consists of a transparent polymer where silicon dioxide microspheres were randomly distributed. The polymer is 50-μm thick and includes 6% of microspheres. The proposed structure is highly emissive across the entire atmospheric transmission window (8 to 13 μm) because of the phonon enhanced Fröhlich resonances of the microspheres. The average emissivity in the atmospheric window is  $\epsilon = 0.93$  [19], or 0.86 [93]. High reflectivity in the shortwave range, is achieved by using a metal mirror [63,82,93], like Al or Ag, with a reflectivity close to 0.96 [82], or a layer of acrylic resin embedded with TiO<sub>2</sub> nanoparticles of 0.2 μm diameter with a reflectivity around to 0.9. Experimental and theoretical characterization of the polymer based radiators, revealed a high daytime net cooling potential varying between 93 W/m<sup>2</sup> [82,93], to 100 W/m<sup>2</sup> [40]. The theoretically estimated daytime temperature depression of the radiations varies between 6 °C below the ambient temperature [40], and 12–25 °C [63], while in [93], water was circulated in the radiative structure and was cooled almost 10.6 °C below the ambient temperature.

In [33,38], commercially available spectrally selective polymers composed by coextruded combinations of many bilayers (Giant Birefringent Optics, GBO), are used to achieve daytime radiative

cooling, as is shown in Figure 3i. The used polymer, described in [96], presents a very high reflectivity, close to 100%, in wavelengths between 0.35 to 1.0  $\mu\text{m}$  and a high absorptivity in the infrared spectrum and an average emissivity close to 0.96. When combined with a metal mirror, like Ag, their combined reflectivity in the shortwave range is close to 0.97. The use of a combined GBO polymers with silver mirrors have been experimentally tested in [38], without any convective/conductive protection and is found to achieve under sunny conditions, a surface temperature almost 2  $^{\circ}\text{C}$  below the ambient one. In [33], the radiator was combined with a water-cooling system and it is found that it is able to decrease the temperature of the circulating water up to 5  $^{\circ}\text{C}$  during the daytime.

#### 4.4. Passive Radiative Cooling Systems Using Paints

Passive radiative materials under the form of paints, do not making use of expensive materials like silver while are available in a simple and easy to use a paint format. In [83], a paint format microsphere based photonic random media is proposed for daytime radiative cooling. Low refractive index microspheres of  $\text{SiO}_2$  are used to create a random photonic media of minimum reflectivity to solar radiation. This is achieved by minimizing the photons transport mean free path  $l'$ , beyond which there is no correlation between the light propagation and its direction. Such a minimization is achieved by using two deposition techniques, colloidal sedimentation and spray coating. It is calculated that the optimum diameter of the  $\text{SiO}_2$  microspheres is close to 1.5  $\mu\text{m}$ , a size much different than the 200–250 nm  $\text{TiO}_2$  microspheres, or 50–150  $\mu\text{m}$  hollow  $\text{TiO}_2$  microspheres used in commercial paints. A media composed by 2  $\mu\text{m}$  diameter  $\text{SiO}_2$  microspheres with a filling factor of 0.6, and a thickness of 500  $\mu\text{m}$ , is found to present an absorptivity in the shortwave range of less than 0.03, while its emissivity in the atmospheric window spectrum was higher than 0.95. A radiative cooling component composed of a 700- $\mu\text{m}$  thickness film of 2  $\mu\text{m}$   $\text{SiO}_2$  spheres deposited on a 2.5 cm  $\times$  2.5 cm glass slide painted black, was experimentally tested. The absorptivity of the radiator in the solar spectrum was 0.02. During the daytime, the radiator exhibited almost 12  $^{\circ}\text{C}$  below the ambient temperature and almost 7  $^{\circ}\text{C}$  below commercial reflecting paints. The temperature drop during the night was close to 4  $^{\circ}\text{C}$ .

In [94], a material for passive daytime radiative cooling is proposed. The material is under the form of a paint and can be applied in building structures. It is based on the development of an hierarchically porous poly(vinylidene fluoride-cohexafluoropropene) (P(VdF-HFP)HP) coating. The coating exhibits superior optical properties. Its reflectance in the solar spectrum is close to 0.96 while its emissivity in the atmospheric window is 0.97. The coating is substrate independent. High reflectivity and emissivity are due to the micro- and nano-pores in the coating that are able to backscatter sunlight and enhance thermal emittance. The coating was tested outdoors under the sun and without a convective protection and shown a daytime temperature depression up to 6  $^{\circ}\text{C}$  below the ambient temperature and a net cooling power close to 96  $\text{W}/\text{m}^2$ . The optical and thermal performance of the proposed coating seems to be superior, however deposition of dust and other atmospheric constituents may seriously affect its performance. In parallel, the impact of the coating during the winter and especially during the clear nights may be important, increasing considerably the heating needs.

## 5. Discussion

Advanced radiative cooling structures based on the use of photonic/plasmonic and metamaterial technologies, demonstrate a very high capacity to provide daytime cooling. Innovative radiative structures succeed to cool their surface temperature, under sunny conditions, up to 10  $^{\circ}\text{C}$  below the ambient temperature. Figure 4 shows in a comparative way the measured or computed daytime surface temperature drop below the ambient temperature from all the proposed radiative structures. As shown when the parasitic losses are substantially reduced, then the cooling performance of the radiators is increasing considerably and may reach 40  $^{\circ}\text{C}$  below the ambient temperature [39].

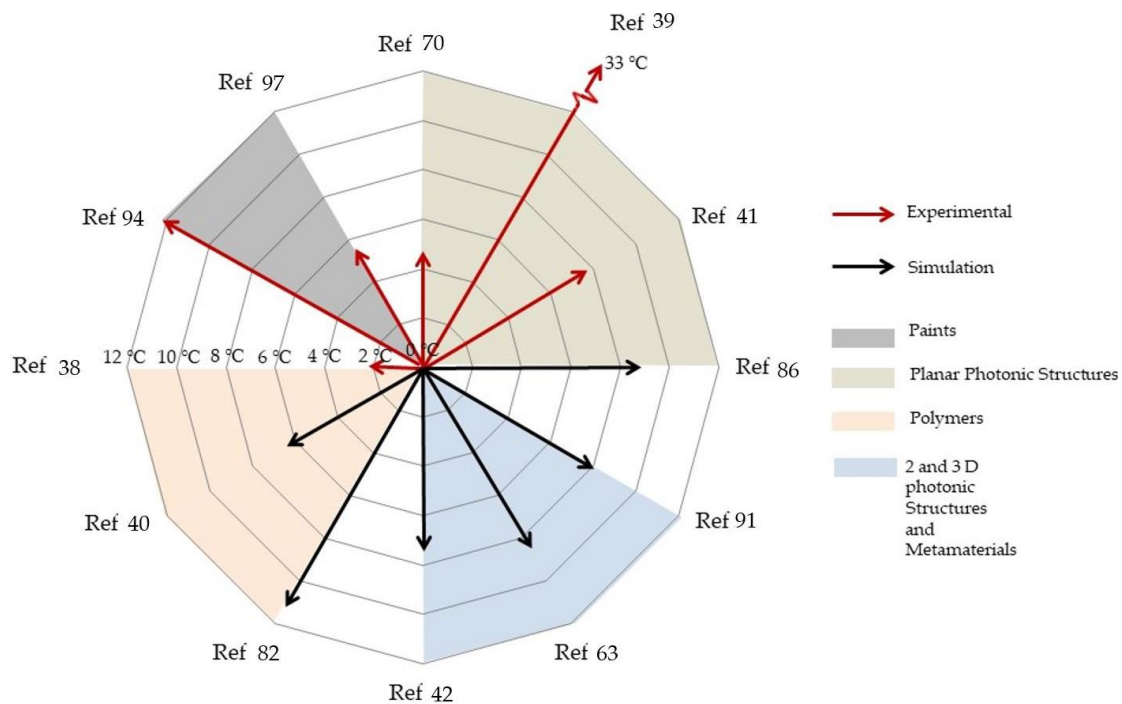


**Figure 4.** Measured and simulated temperature drop below the ambient temperature for selected radiative structures.

The new generation radiative coolers have been already integrated in hydronic air conditioning systems to provide cooling in buildings [33,93]. In all cases, the systems have succeeded to decrease the temperature of the circulating water up to 10.6 °C, below the ambient temperature under sunny conditions. Several studies demonstrated that photonic-based radiative coolers offer an important potential to reduce the cooling demand of buildings. In [33], it is estimated that a hybrid photonic cooling structure can save about 118 MWh per year in Phoenix AZ, while in [97], it is estimated that a similar photonic radiative cooling system can save up to 103 MWh electricity in Miami, 55 MWh in Las Vegas, 50 MWh in Los Angeles, 24 MWh in San Francisco and 43 MWh in Chicago, per year. This corresponds to about 50%, 45%, 65%, 68%, and 55% of the electricity consumed by a Variable Air Volume system in the above five cities respectively.

Space requirements for the radiative collectors may be a concern. According to [93], a photonic air condition system needs almost 13.5 m<sup>2</sup> of radiative collectors to provide a cooling power of 607 W during a sunny summer day. Given that buildings may present a peak cooling power of several kW, considerations about space availability may be a serious problem for the application of the technology. An interesting alternative is to integrate the radiative cooling system on the condenser side of a conventional cooling system to boost its performance, and decrease the required surface [33]. Simulations reported in [33], shown that such a combination may save up to 21% of the cooling load of a two-story building in Las Vegas, NV, USA. The efficiency of a similar approach system using radiative cooling surfaces to replace condensers in conventional or photovoltaic powered air condition systems, is simulated in [98]. It is found that the active use of radiative coolers reduces by 40% the space required for collectors compared to a passive radiative system.

The potential for radiative cooling is seriously reduced in humid climates. High concentration of water vapor in the atmosphere decreases the transparency in the atmospheric window and increases the absorbed infrared radiation at the same wavelengths. It is characteristics [99], that the transmissivity of the atmosphere in the atmospheric window is decreasing by 50% once the concentration of the atmospheric water vapor increases from a small value by 4-fold. Experiments and simulations to measure and estimate the cooling potential of photonic radiative coolers in humid climates shown that in almost all cases, they failed to achieve sub-ambient temperatures during the daytime

period [85,95,100]. A new technique to enhance the performance of photonic radiative coolers under humid climates is proposed in [101]. The method is based on the implementation of an asymmetric electromagnetic window, in the structure of the cooler. Such a component permits the transmission of the outgoing radiation in the atmospheric window but reflects most of the incoming radiation at the same wavelengths. It is estimated that the use of such window could restore the cooling power of the photonic radiative cooler by 57%, in humid climates [101].

Convective losses seriously limit the cooling potential of radiative coolers. To reduce the convective heat exchange with the ambient air, either polyethylene covers were used above the radiator [41,42,83], or a film of ZnSe [39]. Polyethylene and ZnSe, have a high transparency in the atmospheric window and do not restrict considerably the infrared radiation escaping from the radiating structure. However, despite the presence of the cover, significant convective heat exchange happens between the radiator and the surrounding air, while convective and radiative losses from the back side of the radiator are also important. To eliminate most of the parasitic losses, photonic radiators were placed in a vacuum chamber [39]. It was demonstrated that the almost complete elimination of the parasitic losses boosts significantly the performance of the radiator. A giant surface temperature drop below the ambient temperature, 42 °C, was measured during daytime. In contrast, a photonic radiator with almost similar or superior optical characteristics [38], when tested without any convective protection, achieved a temperature drop not higher than 2 °C below the ambient temperature. Given that the optical characteristics of the photonic radiative cooling structures are almost optimized and a further improvement is quite difficult, it seems that most of the future performance improvements may arise from the development of innovative techniques aiming to reduce the parasitic losses of the radiators.

When passive radiative cooling structures are used in buildings, there is a considerable risk to cause undesired cooling during the heating period. Although studies on the potential increase of the heating load because of the passive radiative cooling are not available, serious concerns are expressed on this issue. To face the problem, it is proposed to incorporate in the cooler, switching techniques like materials of temperature depended emissivity to enhance or limit the emitted radiation by the cooling structure according to the needs [88,102]. The integration of a film of a phase change material VO<sub>2</sub> is proposed both in [88,102], to control the emissivity of the radiators. When temperature is above the transition temperature of the VO<sub>2</sub> the emissivity is quite high, while when the temperature is lower, then the emissivity is decreasing considerably.

There are important concerns that the fabrication of the actual photonic nanostructures is very complicated and expensive while present a low scalability potential for building applications. As mentioned in [85], for building radiative cooling purposes, the scalability and the cost seems to be more important than the best optical properties, provided that the cooling potential is quite acceptable.

## 6. Conclusions

Radiative cooling traces many years back. For more than 30 years, several attempts to achieve sub-optimum temperatures under the sun failed because materials do not exhibit enough high solar reflectivity together with a very high emissivity in the atmospheric window. The rapid and impressive development of the photonic nanoscience permitted to develop and demonstrate radiative structures exhibiting surface temperatures much below the ambient one. Several technologies based on metamaterials, planar, 2D or 3D photonic structures, polymeric photonics and paints are developed and tested with impressive results. New generation radiative coolers are already used in association with hydronic air conditioning to provide cooling in real buildings with enough efficiency. Several studies have shown that the energy conservation potential of daytime radiative cooling is considerably high.

Further boosting of the cooling potential of photonic radiative cooling technologies requires a drastic decrease of the parasitic energy associated with the operation of the radiator. The use of vacuum technologies resulted in a giant surface temperature drop below the ambient one. The use of vacuum radiative structures, similar as the vacuum solar collectors may be a priority for the future.

Although the developed photonic technologies have demonstrated a very high cooling potential in arid and dry climates, their use in humid–cloudy zones is seriously limited because of the reduced atmospheric transmissivity in the atmospheric window. The development of asymmetric electromagnetic window techniques seems to be an effective way to overcome the problem and enhance the performance of radiative coolers in humid climates. However, such systems have to be tested in practice and real conditions.

Undesired cooling during the heating period seems to be a serious constraint for the passive radiative cooling technologies integrated in the structure of buildings. The integration of materials having a temperature dependent emissivity is a potential solution to the problem. Preliminary testing shown promising results and further developments are expected soon.

Although the optical characteristics of the proposed structures are extremely high and further improvement may be of quite marginal importance, scalability of the structures is a serious concern. Expensive and complicated fabrication of nanostructures may limit the application of the corresponding technologies, while simpler to fabricate low-cost systems, mainly based on polymeric photonic technologies, seems to present a very high potential for the present and the near future.

**Funding:** This research received no external funding.

**Conflicts of Interest:** The authors declare no conflicts of interest.

## References

1. Founda, D.; Santamouris, M. Synergies between urban heat island and heat waves in Athens (Greece), during an extremely hot summer (2012). *Sci. Rep.* **2017**, *7*, 10973. [[CrossRef](#)] [[PubMed](#)]
2. Santamouris, M. Regulating the damaged thermostat of the cities—Status, impacts and mitigation challenges. *Energy Build.* **2015**, *91*, 43–56. [[CrossRef](#)]
3. Family, R.; Mengüç, M.P. Materials for radiative cooling: A review. *Procedia Environ. Sci.* **2017**, *38*, 752–759. [[CrossRef](#)]
4. Santamouris, M. Cooling the buildings—Past, present and future. *Energy Build.* **2016**, *128*, 617–638. [[CrossRef](#)]
5. BSRIA. *World Market for Air Conditioning*; BSRIA: Bracknell, UK, 2015.
6. Isaac, M.; Van Vuuren, D.P. Modeling global residential sector energy demand for heating and air conditioning in the context of climate change. *Energy Policy* **2009**, *37*, 507–521. [[CrossRef](#)]
7. Santamouris, M. (Ed.) *Cooling Energy Solutions for Buildings and Cities*; World Scientific: Singapore, 2018.
8. McNeil, M.A.L.; Virginie, E. *Future Air Conditioning Energy Consumption in Developing Countries and What Can Be Done about it: The Potential of Efficiency in the Residential Sector*; Lawrence Berkeley National Laboratory: Berkeley, CA, USA, 2008.
9. Silvana Mima, P.C.; Watkiss, P. *The Impacts and Economic Costs of Climate Change on Energy in the European Union: Summary of Sector Results from the Climate Cost Project*; Technical Policy Briefing Note Series; Stockholm Environment Institute: Oxford, UK, 2011.
10. Sivak, M. Potential energy demand for cooling in the 50 largest metropolitan areas of the world: Implications for developing countries. *Energy Policy* **2009**, *37*, 1382–1384. [[CrossRef](#)]
11. Rachel Warren, N.A.; Nicholls, R.; Levy, P.; Price, J. *Understanding the Regional Impacts of Climate Change Research Report Prepared for the Stern Review on the Economics of Climate Change*; Tyndell Centre for Climate Change Research: Norwich, UK, 2006.
12. Hadley, S.W.; Erickson, D.J.; Hernandez, J.L.; Broniak, C.T.; Blasing, T.J. Responses of energy use to climate change: A climate modeling study. *Eophys. Res. Lett.* **2006**, *33*. [[CrossRef](#)]
13. Maryse Labriet, S.R.J.; Vielle, M.; Kanudi, A.; Holden, P.; Edwards, N. *Impacts of Climate Change on Heating and Cooling: A Worldwide Estimate from Energy and Macro-Economic Perspectives*; EPFL: Paris, France, 2013.
14. Silvana Mima, P.C. *Assessment of the Impacts under Future Climate Change on the Energy Systems with the Poles Model*; Fondazione Giorgio Cini: Venice, Italy, 2009.
15. Zhou, Y.; Clarke, L.; Eom, J.; Kyle, P.; Patel, P.; Kim, S.H.; Dirks, J.; Jensen, E.; Liu, Y.; Rice, J.; et al. Modeling the effect of climate change on U.S. state-level buildings energy demands in an integrated assessment framework. *Appl. Energy* **2014**, *113*, 1077–1088. [[CrossRef](#)]

16. Power, E.A. *The European Cold Market, Final Report of the EcoHeatCool Project*; European Union: Brussels, Belgium, 2006.
17. *Annual Energy Outlook 2015*; Energy Information Administration: Washington, DC, USA, 2015.
18. Scott, M.J.; Dirks, J.A.; Cort, K.A. The value of energy efficiency programs for US residential and commercial buildings in a warmer world. *Mitigation Adapt. Strat. Glob. Chang.* **2008**, *13*, 307–339. [[CrossRef](#)]
19. *The Future of Cooling—Opportunities for Energy Efficient Air Conditioning*; International Energy Agency: Paris, France, 2018.
20. Santamouris, M.; Cartalis, C.; Synnefa, A.; Kolokotsa, D. On the impact of urban heat island and global warming on the power demand and electricity consumption of buildings—A review. *Energy Build.* **2015**, *98*, 119–124. [[CrossRef](#)]
21. Santamouris, M. Innovating to zero the building sector in Europe: Minimising the energy consumption, eradication of the energy poverty and mitigating the local climate change. *Sol. Energy* **2016**, *128*, 61–94. [[CrossRef](#)]
22. Karatasou, S.; Laskari, M.; Santamouris, M. Determinants of high electricity use and high energy consumption for space and water heating in European Social Housing: Socio-demographic and building characteristics. *Energy Build.* **2018**, *170*, 107–114. [[CrossRef](#)]
23. Santamouris, M.; Kolokotsa, D. On the impact of urban overheating and extreme climatic conditions on housing, energy, comfort and environmental quality of vulnerable population in Europe. *Energy Build.* **2015**, *98*, 125–133. [[CrossRef](#)]
24. Santamouris, M.; Kapsis, K.; Korres, D.; Livada, I.; Pavlou, C.; Assimakopoulos, M.N. On the relation between the energy and social characteristics of the residential sector. *Energy Build.* **2007**, *39*, 893–905. [[CrossRef](#)]
25. Sakka, A.; Santamouris, M.; Livada, I.; Nicol, F.; Wilson, M. On the thermal performance of low income housing during heat waves. *Energy Build.* **2012**, *49*, 69–77. [[CrossRef](#)]
26. Laboratory, O.R.N. *The Future of Air Conditioning for Buildings*; Navigant Consulting, Inc.: Chicago, IL, USA; Oak Ridge National Laboratory: Oak Ridge, TN, USA, 2016.
27. Santamouris, M.; Synnefa, A.; Karlessi, T. Using advanced cool materials in the urban built environment to mitigate heat islands and improve thermal comfort conditions. *Sol. Energy* **2011**, *85*, 3085–3102. [[CrossRef](#)]
28. Berdahl, P.; Chen, S.S.; Destailats, H.; Kirchstetter, T.W.; Levinson, R.M.; Zalich, M.A. Fluorescent cooling of objects exposed to sunlight—The ruby example. *Sol. Energy Mater. Sol. Cells* **2016**, *157*, 312–317. [[CrossRef](#)]
29. Karlessi, T.; Santamouris, M.; Apostolakis, K.; Synnefa, A.; Livada, I. Development and testing of thermochromic coatings for buildings and urban structures. *Sol. Energy* **2009**, *83*, 538–551. [[CrossRef](#)]
30. Zeyghami, M.; Goswami, D.Y.; Stefanakos, E. A review of clear sky radiative cooling developments and applications in renewable power systems and passive building cooling. *Sol. Energy Mater. Sol. Cells* **2018**, *178*, 115–128. [[CrossRef](#)]
31. Crossley, S.; Mathur, N.D.; Moya, X. New developments in caloric materials for cooling applications. *AIP Adv.* **2015**, *5*, 067153. [[CrossRef](#)]
32. Wang, W.; Fernandez, N.; Katipamula, S.; Alvine, K. Performance assessment of a photonic radiative cooling system for office buildings. *Renew. Energy* **2018**, *118*, 265–277. [[CrossRef](#)]
33. Goldstein, E.A.; Raman, A.P.; Fan, S. Sub-ambient non-evaporative fluid cooling with the sky. *Nat. Energy* **2017**, *2*, 17143. [[CrossRef](#)]
34. Hu, M.; Zhao, B.; Ao, X.; Su, Y.; Wang, Y.; Pei, G. Comparative analysis of different surfaces for integrated solar heating and radiative cooling: A numerical study. *Energy* **2018**, *155*, 360–369. [[CrossRef](#)]
35. Zhao, B.; Hu, M.; Ao, X.; Pei, G. Conceptual development of a building-integrated photovoltaic–radiative cooling system and preliminary performance analysis in Eastern China. *Appl. Energy* **2017**, *205*, 626–634. [[CrossRef](#)]
36. Vall, S.; Castell, A. Radiative cooling as low-grade energy source: A literature review. *Renew. Sustain. Energy Rev.* **2017**, *77*, 803–820. [[CrossRef](#)]
37. Smith, G.; Gentle, A. Radiative cooling: Energy savings from the sky. *Nat. Energy* **2017**, *2*, 17142. [[CrossRef](#)]
38. Gentle, A.R.; Smith, G.B. A Subambient open roof surface under the mid-summer sun. *Adv. Sci.* **2015**, *2*, 1500119. [[CrossRef](#)] [[PubMed](#)]
39. Chen, Z.; Zhu, L.; Raman, A.; Fan, S. Radiative cooling to deep sub-freezing temperatures through a 24-h day–night cycle. *Nat. Commun.* **2016**, *7*, 13729. [[CrossRef](#)] [[PubMed](#)]

40. Huang, Z.; Ruan, X. Nanoparticle embedded double-layer coating for daytime radiative cooling. *Int. J. Heat Mass Transf.* **2017**, *104*, 890–896. [[CrossRef](#)]
41. Kou, J.-L.; Jurado, Z.; Chen, Z.; Fan, S.; Minnich, A.J. Daytime radiative cooling using near-black infrared emitters. *ACS Photon.* **2017**, *4*, 626–630. [[CrossRef](#)]
42. Zou, C.; Ren, G.; Hossain, M.M.; Nirantar, S.; Withayachumnankul, W.; Ahmed, T.; Bhaskaran, M.; Sriram, S.; Gu, M.; Fumeaux, C. metal-loaded dielectric resonator metasurfaces for radiative cooling. *Adv. Opt. Mater.* **2017**, *5*, 1700460. [[CrossRef](#)]
43. Nilsson, T.M.J.; Niklasson, G.A. Radiative cooling during the day: Simulations and experiments on pigmented polyethylene cover foils. *Sol. Energy Mater. Sol. Cells* **1995**, *37*, 93–118. [[CrossRef](#)]
44. Harrison, A.W.; Walton, M.R. Radiative cooling of TiO<sub>2</sub> white paint. *Sol. Energy* **1978**, *20*, 185–188. [[CrossRef](#)]
45. Orel, B.; Gunde, M.K.; Krainer, A. Radiative cooling efficiency of white pigmented paints. *Sol. Energy* **1993**, *50*, 477–482. [[CrossRef](#)]
46. Catalanotti, S.; Cuomo, V.; Piro, G.; Ruggi, D.; Silvestrini, V.; Troise, G. The radiative cooling of selective surfaces. *Sol. Energy* **1975**, *17*, 83–89. [[CrossRef](#)]
47. Tsilingiris, P.T. The total infrared transmittance of polymerised vinyl fluoride films for a wide range of radiant source temperature. *Renew. Energy* **2003**, *28*, 887–900. [[CrossRef](#)]
48. Gupta, A.; Tandon, R.P. Organic–inorganic hybrid polyvinylidene fluoride–Co<sub>0.6</sub>Zn<sub>0.4</sub>Mn<sub>0.3</sub>Fe<sub>1.7</sub>O<sub>4</sub> nanocomposite film with significant optical and magnetodielectric properties. *RSC Adv.* **2015**, *5*, 10110–10118. [[CrossRef](#)]
49. Trombe, F. Perspectives sur l'utilisation des rayonnements solaires et terrestres dans certaines régions du monde. *Rev. Gen. Therm.* **1967**, *6*, 1285.
50. Grenier, P. Réfrigération radiative. Effet de serre inverse. *Rev. Phys. Appl.* **1979**, *14*, 87–90. [[CrossRef](#)]
51. Hossain, M.M.; Gu, M. Radiative cooling: Principles, progress, and potentials. *Adv. Sci.* **2016**, *3*, 1500360. [[CrossRef](#)] [[PubMed](#)]
52. Hjortsberg, A.; Granqvist, C.G. Radiative cooling with selectively emitting ethylene gas. *Appl. Phys. Lett.* **1981**, *39*, 507–509. [[CrossRef](#)]
53. Lushiku, E.M.; Eriksson, T.S.; Hjortsberg, A.; Granqvist, C.G. Radiative cooling to low temperatures with selectively infrared-emitting gases. *Solar Wind Technol.* **1984**, *1*, 115–121. [[CrossRef](#)]
54. Eriksson, T.S.; Lushiku, E.M.; Granqvist, C.G. Materials for radiative cooling to low temperature. *Sol. Energy Mater. Sol. Cells* **1984**, *11*, 149–161. [[CrossRef](#)]
55. Granqvist, C.G.; Hjortsberg, A. Surfaces for radiative cooling: Silicon monoxide films on aluminum. *Appl. Phys. Lett.* **1980**, *36*, 139–141. [[CrossRef](#)]
56. Granqvist, C.G.; Hjortsberg, A. Radiative cooling to low temperatures: General considerations and application to selectively emitting SiO films. *J. Appl. Phys.* **1981**, *52*, 4205–4220. [[CrossRef](#)]
57. Granqvist, C.G.; Hjortsberg, A.; Eriksson, T.S. Radiative cooling to low temperatures with selectivity IR-emitting surfaces. *Thin Solid Films* **1982**, *90*, 187–190. [[CrossRef](#)]
58. Eriksson, T.; Jiang, S.J.; Granqvist, C. Surface coatings for radiative cooling applications—Silicon dioxide and silicon nitride made by reactive RF-sputtering. *Sol. Energy Mater.* **1985**, *12*, 319–325. [[CrossRef](#)]
59. Eriksson, T.S.; Jiang, S.; Granqvist, C.G. Dielectric function of sputter-deposited silicon dioxide and silicon nitride films in the thermal infrared. *Appl. Opt.* **1985**, *24*, 745–746. [[CrossRef](#)] [[PubMed](#)]
60. Liang, Z.; Shen, H.; Li, J.; Xu, N. Microstructure and optical properties of silicon nitride thin films as radiative cooling materials. *Sol. Energy* **2002**, *72*, 505–510. [[CrossRef](#)]
61. Miyazaki, H.; Okada, K.; Jinno, K.; Ota, T.J. Fabrication of radiative cooling devices using Si<sub>2</sub>N<sub>2</sub>O nano-particles. *J. Ceram. Soc. Jpn.* **2016**, *124*, 1185–1187. [[CrossRef](#)]
62. Diatezua, M.; Thiry, D.A.; Dereux, P.; Caudano, A.R. Silicon oxynitride multilayers as spectrally selective material for passive radiative cooling applications. *Sol. Energy Mater. Sol. Cells* **1996**, *40*, 253–259. [[CrossRef](#)]
63. Gentle, A.R.; Smith, G.B. Radiative Heat Pumping from the Earth Using Surface Phonon Resonant Nanoparticles. *Nano Lett.* **2010**, *10*, 373–379. [[CrossRef](#)] [[PubMed](#)]
64. Tazawa, M.; Jin, P.; Tanemura, S. Thin film used to obtain a constant temperature lower than the ambient. *Thin Solid Films* **1996**, *281–282*, 232–234. [[CrossRef](#)]
65. Tazawa, M.; Jin, P.; Yoshimura, K.; Miki, T.; Tanemura, S. New material design with V<sub>1-x</sub>W<sub>x</sub>O<sub>2</sub> film for sky radiator to obtain temperature stability. *Sol. Energy* **1998**, *64*, 3–7. [[CrossRef](#)]

66. Jorgenson, G.V.; Lee, J.C. Doped vanadium oxide for optical switching films. *Sol. Energy Mater. Sol. Cells* **1986**, *14*, 205–214. [[CrossRef](#)]
67. Adachi, S. *Optical Properties of Crystalline and Amorphous Semiconductors*; Springer: Boston, MA, USA, 1999.
68. Berdahl, P. Radiative cooling with MgO and/or LiF layers. *Appl. Opt.* **1984**, *23*, 370–372. [[CrossRef](#)] [[PubMed](#)]
69. Nilsson, N.A.; Eriksson, T.S.; Granqvist, C.G. Infrared-transparent convection shields for radiative cooling: Initial results on corrugated polyethylene foils. *Sol. Energy Mater. Sol. Cells* **1985**, *12*, 327–333. [[CrossRef](#)]
70. Raman, A.P.; Anoma, M.A.; Zhu, L.; Rephaeli, E.; Fan, S. Passive radiative cooling below ambient air temperature under direct sunlight. *Nature* **2014**, *515*, 540. [[CrossRef](#)] [[PubMed](#)]
71. Ali, A.H.H.; Saito, H.; Taha, I.M.S.; Kishinami, K.; Ismail, I.M. Effect of aging, thickness and color on both the radiative properties of polyethylene films and performance of the nocturnal cooling unit. *Energy Conv. Manag.* **1998**, *39*, 87–93. [[CrossRef](#)]
72. Gentle, A.R.; Dybdal, K.L.; Smith, G.B. Polymeric mesh for durable infra-red transparent convection shields: Applications in cool roofs and sky cooling. *Sol. Energy Mater. Sol. Cells* **2013**, *115*, 79–85. [[CrossRef](#)]
73. Nilsson, T.M.J.; Niklasson, G.A.; Granqvist, C.G. A solar reflecting material for radiative cooling applications: ZnS pigmented polyethylene. *Sol. Energy Mater. Sol. Cells* **1992**, *28*, 175–193. [[CrossRef](#)]
74. Niklasson, G.A.; Eriksson, T.S. Radiative Cooling with Pigmented Polyethylene Foils. In Proceedings of the 1988 International Congress on Optical Science and Engineering, Hamburg, Germany, 24–26 April 1988; p. 11.
75. Mastai, Y.; Diamant, Y.; Aruna, S.T.; Zaban, A. TiO<sub>2</sub> Nanocrystalline Pigmented Polyethylene Foils for Radiative Cooling Applications: Synthesis and Characterization. *Langmuir* **2001**, *17*, 7118–7123. [[CrossRef](#)]
76. Dobson, K.D.; Hodes, G.; Mastai, Y. Thin semiconductor films for radiative cooling applications. *Sol. Energy Mater. Sol. Cells* **2003**, *80*, 283–296. [[CrossRef](#)]
77. Naghshine, B.B.; Saboonchi, A. Optimized thin film coatings for passive radiative cooling applications. *Opt. Commun.* **2018**, *410*, 416–423. [[CrossRef](#)]
78. Benlattar, M.; Oualim, E.M.; Harmouchi, M.; Mouhsen, A.; Belafhal, A. Radiative properties of cadmium telluride thin film as radiative cooling materials. *Opt. Commun.* **2005**, *256*, 10–15. [[CrossRef](#)]
79. Benlattar, M.; Oualim, E.M.; Mouhib, T.; Harmouchi, M.; Mouhsen, A.; Belafhal, A. Thin cadmium sulphide film for radiative cooling application. *Opt. Commun.* **2006**, *267*, 65–68. [[CrossRef](#)]
80. Engelhard, T.; Jones, E.D.; Viney, I.; Mastai, Y.; Hodes, G. Deposition of tellurium films by decomposition of electrochemically-generated H<sub>2</sub>Te: Application to radiative cooling devices. *Thin Solid Films* **2000**, *370*, 101–105. [[CrossRef](#)]
81. Mouhib, T.; Mouhsen, A.; Oualim, E.M.; Harmouchi, M.; Vigneron, J.P.; Defrance, P. Stainless steel/tin/glass coating as spectrally selective material for passive radiative cooling applications. *Opt. Mater.* **2009**, *31*, 673–677. [[CrossRef](#)]
82. Zhai, Y.; Ma, Y.; David, S.N.; Zhao, D.; Lou, R.; Tan, G.; Yang, R.; Yin, X. Scalable-manufactured randomized glass-polymer hybrid metamaterial for daytime radiative cooling. *Science* **2017**. [[CrossRef](#)] [[PubMed](#)]
83. Atigyanun, S.; Plumley, J.B.; Han, S.J.; Hsu, K.; Cytrynbaum, J.; Peng, T.L.; Han, S.M.; Han, S.E. Effective radiative cooling by paint-format microsphere-based photonic random media. *ACS Photonics* **2018**, *5*, 1181–1187. [[CrossRef](#)]
84. Narayanaswamy, A.; Mayo, J.; Canetta, C. Infrared selective emitters with thin films of polar materials. *Appl. Phys. Lett.* **2014**, *104*, 183107. [[CrossRef](#)]
85. Bao, H.; Yan, C.; Wang, B.; Fang, X.; Zhao, C.Y.; Ruan, X. Double-layer nanoparticle-based coatings for efficient terrestrial radiative cooling. *Sol. Energy Mater. Sol. Cells* **2017**, *168*, 78–84. [[CrossRef](#)]
86. Kecebas, M.A.; Menguc, M.P.; Kosar, A.; Sendur, K. Passive radiative cooling design with broadband optical thin-film filters. *J. Quant. Spectrosc. Radiat. Transf.* **2017**, *198*, 179–186. [[CrossRef](#)]
87. Hervé, A.; Drevillon, J.; Ezzahri, Y.; Joulain, K. Radiative cooling by tailoring surfaces with microstructures. *arXiv* **2018**, arXiv:1802.02067.
88. Ono, M.; Chen, K.; Li, W.; Fan, S. Self-adaptive radiative cooling based on phase change materials. *Opt. Express* **2018**, *26*, A777–A787. [[CrossRef](#)] [[PubMed](#)]
89. Rephaeli, E.; Raman, A.; Fan, S. Ultrabroadband photonic structures to achieve high-performance daytime radiative cooling. *Nano Lett.* **2013**, *13*, 1457–1461. [[CrossRef](#)] [[PubMed](#)]
90. Hossain, M.M.; Jia, B.; Gu, M. A metamaterial emitter for highly efficient radiative cooling. *Adv. Opt. Mater.* **2015**, *3*, 1047–1051. [[CrossRef](#)]

91. Yang, Y.; Taylor, S.; Alshehri, H.; Wang, L. Wavelength-selective and diffuse infrared thermal emission mediated by magnetic polaritons from silicon carbide metasurfaces. *Appl. Phys. Lett.* **2017**, *111*, 051904. [[CrossRef](#)]
92. Wu, D.; Liu, C.; Xu, Z.; Liu, Y.; Yu, Z.; Yu, L.; Chen, L.; Li, R.; Ma, R.; Ye, H. The design of ultra-broadband selective near-perfect absorber based on photonic structures to achieve near-ideal daytime radiative cooling. *Mater. Des.* **2018**, *139*, 104–111. [[CrossRef](#)]
93. Zhao, D.; Aili, A.; Zhai, Y.; Lu, J.; Kidd, D.; Tan, G.; Yin, X.; Yang, R. Subambient cooling of water: Toward real-world applications of daytime radiative cooling. *Joule* **2018**. [[CrossRef](#)]
94. Mandal, J.; Fu, Y.; Overvig, A.; Jia, M.; Sun, K.; Shi, N.; Zhou, H.; Xiao, X.; Yu, N.; Yang, Y. Hierarchically porous polymer coatings for highly efficient passive daytime radiative cooling. *Science* **2018**. [[CrossRef](#)] [[PubMed](#)]
95. Suichi, T.; Ishikawa, A.; Hayashi, Y.; Tsuruta, K. Performance limit of daytime radiative cooling in warm humid environment. *AIP Adv.* **2018**, *8*, 055124. [[CrossRef](#)]
96. Weber, M.F.; Stover, C.A.; Gilbert, L.R.; Nevitt, T.J.; Ouderirk, A.J. Giant birefringent optics in multilayer polymer mirrors. *Science* **2000**, *287*, 2451. [[CrossRef](#)] [[PubMed](#)]
97. Fernandez, N.; Wang, W.; Alvine, K.J.; Katipamula, S. *Energy Savings Potential of Radiative Cooling Technologies*; United States Dept. of Energy: Washington, DC, USA, 2015.
98. Bergman, T.L. Active daytime radiative cooling using spectrally selective surfaces for air conditioning and refrigeration systems. *Sol. Energy* **2018**, *174*, 16–23. [[CrossRef](#)]
99. Observatory, G. Infrared Atmospheric Transmission Spectrum at Mauna Kea. Available online: <https://www.gemini.edu/sciops/telescopes-and-sites/observing-condition-constraints/ir-transmission-spectra> (accessed on 20 October 2018).
100. Tso, C.Y.; Chan, K.C.; Chao, C.Y.H. A field investigation of passive radiative cooling under Hong Kong's climate. *Renew. Energy* **2017**, *106*, 52–61. [[CrossRef](#)]
101. Wong, R.Y.M.; Tso, C.Y.; Chao, C.Y.H.; Huang, B.; Wan, M.P. Ultra-broadband asymmetric transmission metallic gratings for subtropical passive daytime radiative cooling. *Sol. Energy Mater. Sol. Cells* **2018**, *186*, 330–339. [[CrossRef](#)]
102. Gentle, A.; Tai, M.; White, S.; Arnold, M.; Cortie, M.; Smith, G. Design, control, and characterisation of switchable radiative cooling. In Proceedings of the SPIE Optical Engineering + Applications, San Diego, CA, USA, 19–23 August 2018; p. 10.



© 2018 by the authors. Licensee MDPI, Basel, Switzerland. This article is an open access article distributed under the terms and conditions of the Creative Commons Attribution (CC BY) license (<http://creativecommons.org/licenses/by/4.0/>).